

## Synthesis and Phase Transformation of $\text{In}_2\text{Se}_3$ and $\text{CuInSe}_2$ Nanowires

Hailin Peng,<sup>†</sup> David T. Schoen,<sup>†</sup> Stefan Meister,<sup>†</sup> Xiao Feng Zhang,<sup>‡</sup> and Yi Cui<sup>\*†</sup>

Department of Materials Science and Engineering, Stanford University, Stanford, California 94305, and Electron Microscope Division, Hitachi High Technologies America, Inc., 5100 Franklin Drive, Pleasanton, California 94588

Received October 17, 2006; E-mail: yicui@stanford.edu

Bulk and thin films of III–VI and I–III–VI semiconductors such as  $\text{In}_2\text{Se}_3$  (IS),<sup>1</sup>  $\text{CuInSe}_2$  (CIS)<sup>2</sup> and  $\text{CuGaSe}_2$ <sup>3</sup> have been actively studied for photovoltaic applications. Among them, polycrystalline thin films of  $\text{CuIn}_x\text{Ga}_{1-x}\text{Se}_2$  (CIGS) have been demonstrated to have a high-power efficiency of 19.2%,<sup>4</sup> which even outperforms the best single crystalline devices.<sup>5</sup> This extraordinary performance was proposed to be caused by a hole energy barrier at grain boundaries for preventing electron-hole recombination,<sup>6,7</sup> although this hypothesis is still under question.<sup>8</sup> In addition, the high efficiency is also attributed to the formation of random p–n junctions distributed in compositionally inhomogeneous polycrystalline thin films.<sup>9</sup> Nanowire (NW) morphology of I–III–VI chalcopyrite materials can provide a well-defined nanoscale domain with clearly identifiable “grain boundaries” for studying these effects. Aligned NWs with a controllable composition modulation can afford ordered p–n junctions and continuous charge carrier transport pathways without deadends, which is an advantage over the random p–n junctions. Therefore, NW solar cells<sup>10</sup> might provide an even higher efficiency. The promise will not be fulfilled without a method for fabricating the required NW structures. Herein, we report the synthesis of IS and CIS single crystalline NWs via a Au-catalyzed vapor–liquid–solid (VLS) growth. We demonstrate the temperature-induced reversible superlattice transformation in IS NWs. We also show that the crystal structure of CIS NWs has dependence on Cu concentration.

A solvothermal method was used previously for producing CIS nanowiskers and nanoparticles although their morphology and crystallinity are ill-defined.<sup>11</sup> Solution colloidal synthesis was used to produce  $\text{AgInSe}_2$  nanorods and nanoparticles with small aspect ratios less than 5.<sup>12</sup> We exploit a VLS growth<sup>13–15</sup> because this method has been shown to be among the most powerful ones for predictably synthesizing single-crystalline NW structures with a size, position, and orientation control.

The synthesis of IS and CIS NWs has been carried out in a similar way as that in our previous studies<sup>16</sup> (Supporting Information). In a tube furnace, a carrier gas transports the vapor of  $\alpha$ -phase IS or chalcopyrite-type CIS downstream. Gold colloids dispersed on Si substrates were used as VLS catalysts. Typical synthesis conditions are pressure = 50 Torr, temperature = 700 °C, time = 5 h, and gas flow = 120 sccm. To controllably adjust the Cu concentration in CIS NWs, additional CuI powder was placed upstream. The NWs were characterized in an FEI Sirion scanning electron microscope (SEM), a Hitachi 300 kV H-9500 and a Philips CM20 transmission electron microscope (TEM), and by energy dispersive X-ray spectrometry (EDX).

Figure 1a shows a typical SEM image of as-grown IS NWs. The NW diameters range from 20 to 150 nm with lengths up to over 100  $\mu\text{m}$ . The TEM image (Figure 1b) demonstrates that most NWs have a uniform diameter along their length and have a particle

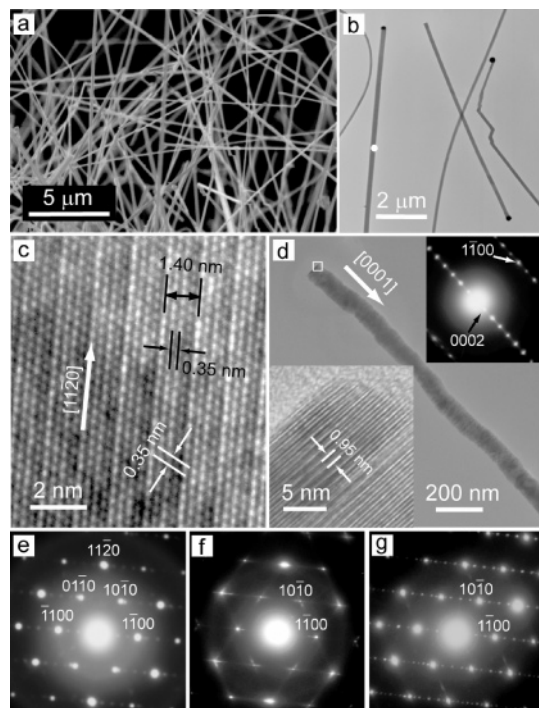


**Figure 1.** (a) SEM image of IS NWs on a Si  $\langle 111 \rangle$  substrate. (b) TEM image of IS NWs. (c) HRTEM image of the IS NW (white spot in panel b). (d) TEM image of a curly IS NW. The insets show a HRTEM image recorded from the area indicated by the white rectangle and the corresponding SAED pattern. (e–g) SAED patterns of the IS NW recorded at 22, 267, and 23 °C, sequentially (white spot in panel b).

at the tip, suggesting a VLS growth mechanism. EDX spectra (Figure S1 in Supporting Information) reveal the presence of Au in the tip, while the NW consists of In and Se with an atomic ratio of 2:3 confirming the chemical composition of  $\text{In}_2\text{Se}_3$ . High-resolution TEM (HRTEM) (Figure 1c) and selected-area electron diffraction (SAED) (Figure 1e) of the typical IS NWs show the clearly identified hexagonal lattice planes with lattice spacing of 0.35 nm (Figure 1c), corresponding to the (1–100) plane of the hexagonal  $\alpha$ - $\text{In}_2\text{Se}_3$  (JCPDS-00-034-1279) looking along the [0001] zone axis. The NW growth direction is [1–20], confirmed by the corresponding SAED pattern (Figure 1e). Most interestingly, a one-dimensional superlattice perpendicular to the NW growth direction is observed in most of the IS NWs at room temperature (Figure 1c). The superlattice has a periodicity of 1.40 nm and one period consists of four (1–100) planes. The presence of the superlattice is confirmed by the SAED pattern (Figure 1e), in which the distance between two basic spots is subdivided into four equal parts along the [1–100] direction. We also noted the eight-plane periodicity (twice of four-planes) in our TEM studies.

Superlattices were previously observed in thin film IS with a periodicity of eight or nine (1–100) planes at temperatures between

<sup>†</sup> Stanford University.

<sup>‡</sup> Hitachi High Technologies America, Inc.

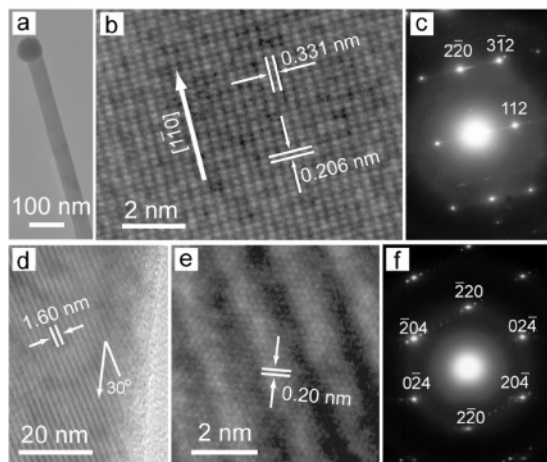


**Figure 2.** (a) TEM image of a Cu-rich CIS NW with a Au particle. (b and c) HRTEM image and SAED pattern of the NW in panel a, respectively. (d) TEM image of a Cu-deficient CIS NW. (e and f) HRTEM image and SAED pattern of the NW in panel d, respectively.

60 and 200 °C.<sup>17</sup> This is the first time that IS superlattices have been observed at room temperature. The presence of four-plane periodicity in NW structures has not been observed in thin films probably because of the nanoscale size effect and needs further investigation. Our extensive in-situ TEM studies show that the IS NWs undergo a reversible superlattice phase transformation at ~200 °C. This temperature is consistent with previous thin-film studies.<sup>17</sup> On heating, the NW superstructure disappears at 200 °C, indicated by the SAED pattern (Figure 1f and Figure S3 in Supporting Information). The diffuse streaks are observed along the hexagonal array of the basic spots, which is attributed to anisotropic transverse acoustic phonons upon phase transformation.<sup>17</sup> Cooling NWs to room temperature can bring back the superlattices with four- or eight-plane periodicity (Figure 1g) although this transformation takes place over a long time of tens of minutes to hours. The superlattice formation mechanism might be the freeze-in of a particular vibration mode<sup>17</sup> and requires future studies.

In addition to the dominating [11–20] growth direction, a small fraction (~10%) of IS NWs can grow along the [0001] direction. The HRTEM image (Figure 1d, bottom inset) displays alternating bright and dark fringes with a ~0.95 nm periodicity, corresponding to the (0002) planes of hexagonal IS. The SAED pattern (Figure 1d, top inset) indicates that the growth direction is [0001] without superlattice structure. The IS structure can be viewed as layers packing along the [0001] axis via a weak van der Waals interaction and each layer consists of Se–In–Se–In–Se.<sup>18</sup> The [0001] oriented NWs show a rough sidewall surface and flat end (Figure 1d), consistent with the bonding nature of IS. The as-grown [0001] IS NWs were found to lie flat on the Si substrate while the [11–20] NWs stand out. This suggests that the interaction between the NW side wall and the substrate might be an important factor to determine the energetics of the VLS growth.

Cu-rich CIS NWs have been synthesized with CIS and additional CuI powder as precursors. SEM images show that CIS NWs have a similar morphology as that of IS NWs with a diameter of 20–200 nm and length up to tens of  $\mu\text{m}$  (Figure S4 in Supporting Information). Figure 2a shows a TEM image of a CIS NW with a Au particle at the end (Figure S5 in Supporting Information). The NW consists of Cu, In, and Se with an atomic ratio of 1.04:0.92:2.04 (26%:23%:51%). Statistical examinations of a large number of NWs reveal that the compositions of the NWs are close to

CuInSe<sub>2</sub> slightly rich in Cu. HRTEM images (Figure 2b) of CIS NWs show a single-crystalline structure. The spacing of the lattice planes parallel and perpendicular to the long axis of the NW are 0.331 and 0.206 nm, consistent with the (112) and (2–20) planes of the CIS chalcopyrite structure, respectively. The corresponding SAED pattern (Figure 2c) is indexed along the [11–1] zone axis. The NW growth direction is along [1–10], consistent with HRTEM studies. Detailed TEM studies on a large number of CIS NWs show that they lay down on carbon supporting films with different zone axes parallel to the electron beam (Figure S7–9 in Supporting Information). All of the CIS NWs show the [1–10] growth direction without exception.

The ability to control both the Cu-rich and Cu-deficient CIS is important for solar cell p–n junction formation. We can synthesize Cu-deficient CIS NWs with CIS precursors only. The EDX data show that NWs consist of Cu, In, and Se with an atomic ratio of 0.60:1.36:2.04 (15%:34%:51%), in which the amount of Cu is clearly less than In (Figure S6 in Supporting Information). Cu-deficient CIS NWs also have the CIS chalcopyrite structure but with the presence of superlattice structures, the characteristic of the IS NWs. Figure 2d shows a typical TEM image of the Cu-deficient CIS NWs. A 1.60 nm periodic superstructure is formed along the direction having a ~30° angle to the NW long axis. The HRTEM image and corresponding SAED pattern (Figure 2e and f) reveal that the hexagonal lattice of the CIS chalcopyrite phase forms a one-dimensional 8-fold superstructure along the [01–2] direction. The data suggest that the Cu-deficient CIS NWs have the transition-state characteristics between CIS and IS NWs.

**Acknowledgment.** Y.C. acknowledges support from Stanford New Faculty Startup Fund, NMTRI, CIS, and CPN fund. D.T.S. would like to thank NDSEG Fellowship support.

**Supporting Information Available:** EDX and HRTEM of IS NWs, synthesis and XRD of the CIS precursor, SEM image, TEM images, and EDX data of CIS NWs. This material is available free of charge via the Internet at <http://pubs.acs.org>.

## References

- (1) Kwon, S. H.; Ahn, B. T.; Kim, S. K.; Yoon, K. H.; Song, J. *Thin Solid Films* **1998**, *323*, 265.
- (2) Rockett, A.; Birkmire, R. W. *J. Appl. Phys.* **1991**, *70*, R81.
- (3) Saad, M.; Riaz, H.; Bucher, E.; Lux-Steiner, M. *Ch. Appl. Phys. A* **1996**, *62*, 181.
- (4) Champness, C. H. Proceedings of the 29th IEEE Conference. Piscataway, NY, 2002; p 732.
- (5) Ramanathan, K.; Contreras, M. A.; Perkins, C. L.; Asher, S.; Hasoon, F. S.; Keane, J.; Young, D.; Romero, M.; Metzger, W.; Noufi, R.; Ward, J.; Duda, A. *Prog. Photovoltaics* **2003**, *11*, 225.
- (6) Persson, C.; Zunger, A. *Phys. Rev. Lett.* **2003**, *91*, 266401.
- (7) Hetzer, M. J.; Strzhemechny, Y. M.; Gao, M.; Contreras, M. A.; Zunger, A.; Brillson, L. *J. Appl. Phys. Lett.* **2005**, *86*, 162105.
- (8) Yan, Y.; Noufi, R.; Al-Jassim, M. M. *Phys. Rev. Lett.* **2006**, *96*, 205501.
- (9) Yan, Y.; Noufi, R.; Jones, K. M.; Ramanathan, K.; Al-Jassim, M. M.; Stanbery, B. *J. Appl. Phys. Lett.* **2005**, *87*, 121904.
- (10) Law, M.; Greene, L. E.; Johnson, J. C.; Saykally, R.; Yang, P. *Nat. Mater.* **2005**, *4*, 455.
- (11) Gou, X.; Cheng, F.; Shi, Y.; Zhang, L.; Peng, S.; Chen, J.; Shen, P. *J. Am. Chem. Soc.* **2006**, *128*, 7222.
- (12) Ng, M. T.; Boothroyd, C. B.; Vittal, J. J. *J. Am. Chem. Soc.* **2006**, *128*, 7118.
- (13) Lieber, C. M. *MRS Bull.* **2003**, *28*, 486.
- (14) Yang, P. *MRS Bull.* **2005**, *30*, 85.
- (15) Björk, M. T.; Ohlsson, B. J.; Sass, T.; Persson, A. I.; Thelander, C.; Magnusson, M. H.; Deppert, K.; Wallenberg, L. R.; Samuelson, L. *Appl. Phys. Lett.* **2002**, *80*, 1058.
- (16) Meister, S.; Peng, H.; McIlwrath, K.; Jarausch, K.; Zhang, X. F.; Cui, Y. *Nano Lett.* **2006**, *6*, 1514.
- (17) Van Landuyt, J.; Van Tendeloo, G.; Amelinckx, S. *Phys. Stat. Sol. A* **1975**, *30*, 299.
- (18) Ye, J.; Soeda, S.; Nakamura, Y.; Nittono, O. *Jpn. J. Appl. Phys.* **1998**, *37*, 4264.

JA067436K